

Metabolic Design of Macroscopic Models: Application to CHO cells

A. Provost and G. Bastin

Applied Mathematics Department
Université catholique de Louvain
Louvain-la-Neuve Belgium
provost,bastin@auto.ucl.ac.be

S.N. Agathos

Unit of Bioengineering
Université catholique de Louvain
Louvain-la-Neuve Belgium
agathos@gebi.ucl.ac.be

Y.-J. Schneider

Lab. of Cellular Biochemistry
Université catholique de Louvain
Louvain-la-Neuve Belgium
yjs@bioc.ucl.ac.be

Abstract—The aim of this paper is to present a systematic methodology to design macroscopic models for cell cultures based upon metabolic networks. The cell life is seen as a succession of phases. During each phase, a metabolic network represents the set of reactions occurring in the cell. Then, through the use of the Elementary Flux Modes, these metabolic networks are used to derive macroscopic reactions linking the extracellular substrates and products. On this basis, as many separate models are obtained as there are phases. Then, a complete model is obtained by smoothly switching from model to model. This is illustrated with batch cultures of Chinese Hamster Ovary (CHO) cells.

I. INTRODUCTION

The metabolism of a cell line is usually represented by a metabolic network (see Fig. 1 for an illustration) which graphically depicts the reactions taking place within the cell as well as the reactions with its environment. It is a well-known fact that the metabolic routes change during the cell life mainly depending on the availability of the substrates. The aim of this paper is to present a systematic methodology to design macroscopic models for cell cultures based upon metabolic networks. We shall present a global model which is able to describe the cell dynamics for the whole duration of the cell life. The model will take into account the changes of the metabolism during the cell life and involve, in a unified framework, the three main successive phases of the cell life, namely the growth phase, the "transition" phase and the death phase. According to experimental observations a specific and different metabolic map will be used for each phase. The methodology will be illustrated with the particular case of CHO cells.

In the first section, the passage from a metabolic network to a general macroscopic model is described. It is shown how the elementary flux modes which are obtained from the convex basis of the network stoichiometric matrix (see [1] for details) are transformed into a set of macroscopic reactions involving only measurable substrates and products present in the culture medium. Then the set of reactions is further reduced by aggregating the macroscopic reactions that share the same reactants. Finally, a mass balance dynamical model is derived and validated with the experimental data. This methodology has already been used by the authors to obtain a model for the growth phase (see [2]). Our contribution in this paper is to show how the methodology can be extended, in a unified and systematic way, to the other phases of the cell life (transition and death phases). Three separate models

are obtained each of them based on a metabolic network specific to its own phase. Finally the complete model is build up by using the three separate models in their respective time interval, smoothly switching from model to model, on the basis of the availability of the two main substrates: Glucose and Glutamine.

II. PRINCIPLES OF METABOLIC DESIGN OF MACROSCOPIC MODELS

When conceiving a macroscopic model, the cell mass in the bioreactor is viewed as a black box device that catalyses the conversion of substrates into products (see Fig. 2). The overall conversion mechanism is described by a rather small set of key macroscopic reactions that directly connect the substrates to the products. In this paper we are concerned with the design of such macroscopic models when measurements of extra-cellular substrates and products in the culture medium are the only available data besides measurements of the biomass (see also [3] for a different approach). It is assumed that the cells are cultivated in batch mode in a stirred tank reactor. The dynamics of substrates and products are described by the following basic differential equations:

$$\begin{aligned}\dot{s} &= -v_s X \\ \dot{p} &= v_p X\end{aligned}\quad (1)$$

where X is the biomass concentration, s is the vector of substrate concentrations, p is the vector of product concentrations, v_s is the vector of specific uptake rates and v_p is the vector of specific excretion rates.

Obviously, the specific rates v_s and v_p are not independent: they are quantitatively related through the intracellular metabolism (see Fig. 1) represented by a metabolic network. A metabolic network is a directed hypergraph encoding a (possibly very large) set of elementary biochemical reactions taking place in the cell. In the graph, the nodes represent the involved metabolites and the arcs represent the fluxes.

In order to explicit the link between uptake and excretion rates, the quasi steady-state viewpoint of metabolic flux analysis (MFA) is adopted. This means that for each intermediate metabolite, it is assumed that the net sum of production and consumption fluxes, weighted by their stoichiometric coefficients, is zero. This is expressed by an algebraic relation:

$$Nv = 0 \quad (2)$$

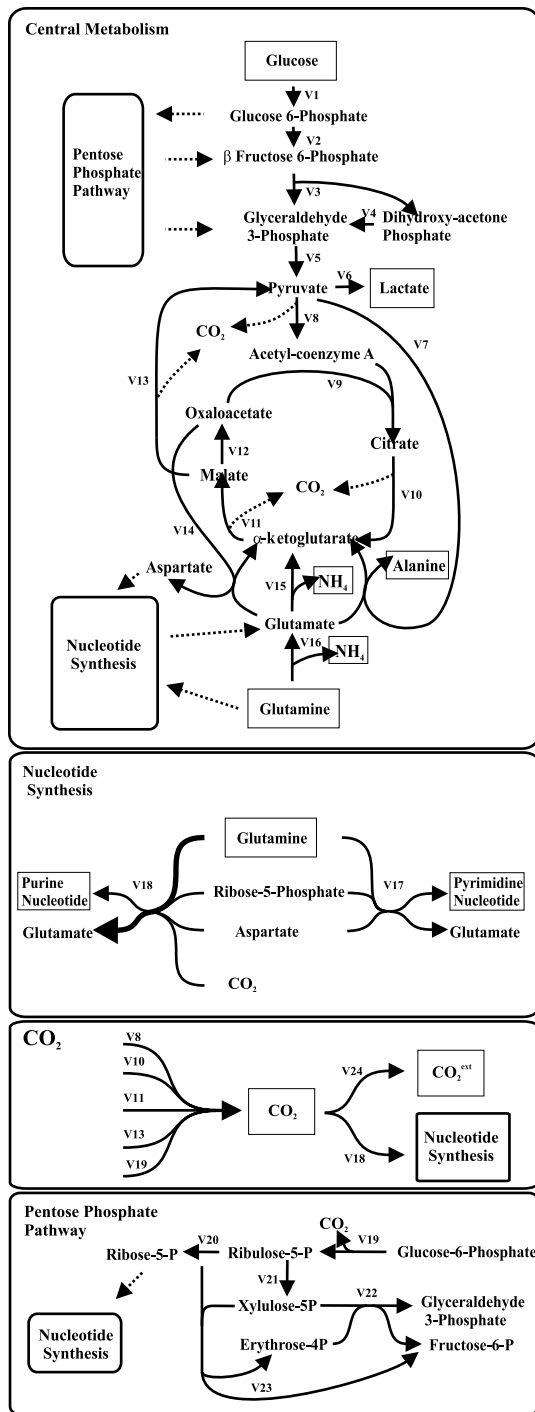


Fig. 1. Metabolic network for the growth of CHO-320 cells. Bold arrows stand for double arrows.

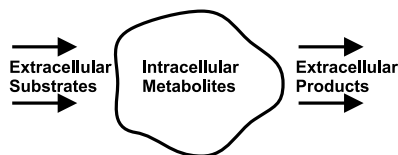


Fig. 2. Cells seen as reactors converting extracellular substrates into extracellular products.

where v is the vector of the fluxes v_j and $N = [n_{ij}]$ is the stoichiometric matrix of the metabolic network. More precisely, the flux v_j denotes the rate of reaction j and a non-zero n_{ij} is the stoichiometric coefficient of metabolite i in reaction j . The quasi steady-state approximation is justified because the intracellular metabolic transients are much faster than the process transients as represented by equations (1).

By definition the specific uptake and excretion rates v_s and v_p are linear combinations of some of the metabolic fluxes. This is expressed by defining appropriate matrices N_s and N_p such that:

$$v_s = N_s v \quad v_p = N_p v. \quad (3)$$

As indicated above, our aim is to design a reduced-order macroscopic model in order to link the extracellular substrates and products in a metabolic meaningful way.

The first stage is to compute the elementary flux modes (EFM) which are the non-negative vectors of the convex basis of the stoichiometric matrix N . Therefore they are the columns of a non-negative matrix E such that $NE = 0$.

Biochemically speaking, the elementary flux modes encode the simplest metabolic routes that connect the substrates to the products. More precisely, an elementary flux mode is a sequence of biochemical reactions starting with one or several substrates and ending with one or several products. Since the intermediate reactions are assumed to be at quasi steady-state, a macroscopic reaction is then readily defined from an elementary flux mode by considering only the initial substrates and the final products. The stoichiometric matrix K of the set of macroscopic reactions can be shown to be given by the following expression:

$$K = \begin{pmatrix} -N_s \\ N_p \end{pmatrix} E. \quad (4)$$

Let ξ denote the vector of extracellular species concentrations:

$$\xi = \begin{pmatrix} s \\ p \end{pmatrix}.$$

Then the dynamical model of the extracellular species governed by the macroscopic reactions in the bioreactor is naturally written as:

$$\dot{\xi} = KwX \quad (5)$$

where w represents the vector of the specific rates of the macroscopic reactions. From (4) and (5), we obtain:

$$\dot{\xi} = KwX = \begin{pmatrix} -N_s \\ N_p \end{pmatrix} EwX. \quad (6)$$

Moreover, from (1) and (3), we obtain:

$$\dot{\xi} = \begin{pmatrix} -N_s \\ N_p \end{pmatrix} vX.$$

Thus, there is a linear relation between the intracellular fluxes v and the macroscopic reaction rates w :

$$v = Ew$$

In biochemical terms, this means that the fluxes v_i are positive linear combinations of the specific rates w_i associated with the elementary flux modes of the metabolic network.

Because the number of elementary flux modes may be too large for a practical engineering utilisation, we suggest a further relevant model reduction by aggregation of the macroscopic reactions that share the same substrates. This is expressed by defining a reduced set of aggregated reactions which are weighted sums of the macroscopic reactions. The aggregation mechanism is formulated as follows:

$$w = Ar$$

where r denotes the vector of the specific reaction rates of the aggregated reactions and A is the aggregation matrix with entries α_{ij} such that $0 \leq \alpha_{ij} \leq 1$ and $\sum_i \alpha_{ij} = 1$ (α_{ij} is the weighting factor of macroscopic reaction i in aggregated reaction j).

The reduced model is therefore written under the following form:

$$\dot{\xi} = LrX$$

with $L = KA$ the pseudo-stoichiometric matrix of the aggregated macroscopic reactions. Obviously this reduced model makes sense only if the matrix L is structurally identifiable. In the remainder of this paper, we shall apply this modelling methodology to CHO cells and discuss the structural identifiability conditions on L in this context.

III. APPLICATION TO CHO CELLS

In order to illustrate and motivate the methodology that we have presented above, we consider the example of CHO cells cultivated in batch mode in stirred flasks. The measured extracellular species are two substrates (Glucose and Glutamine) and three excreted products (Lactate, Ammonia, Alanine). The experimental data collected during three experiments are shown in Fig. 3. For this modelling study, three successive phases will be considered: the growth phase (marked by + in Fig. 3), the transition phase (marked by o) and the death phase (marked by x).

A. The Growth Phase Model

The metabolic network considered for the growth phase is presented in Fig. 1. This metabolic network describes only the part of the metabolism concerned with the utilisation of the two main energetic nutrients (Glucose and Glutamine). The metabolism of the amino-acids provided by the culture medium is not considered. It is assumed that a part of the Glutamine is used for the making of purine and pyrimidine nucleotides but is not directly involved in the formation of proteins. This is obviously a simplifying assumption that could be discussed. It must however be mentioned that this assumption appears to be quite acceptable since a metabolic flux analysis (reported in reference [2]) based on the network of Fig. 1 gives a production of nucleotides which is in agreement with the data of the literature. Since the goal is to compute the elementary flux modes, all the intermediate species that are not located at branch points are omitted

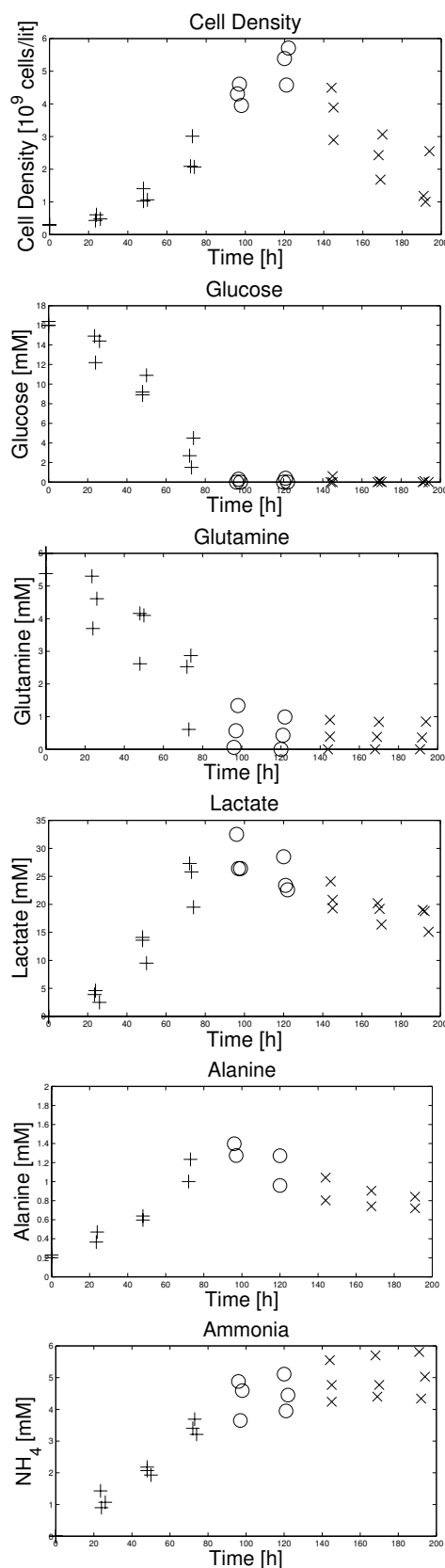


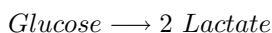
Fig. 3. Biomass production and measured extracellular species for three CHO-320 batch cultures. Growth, transition and death phases data are respectively represented by +, o and x marks.

v_1	v_2	v_3	v_4	v_5	v_6	v_7	v_8	v_9	v_{10}	v_{11}	v_{12}	v_{13}	v_{14}	v_{15}	v_{16}	v_{17}	v_{18}	v_{19}	v_{20}	v_{21}	v_{22}	v_{23}	v_{24}
1	-1	0	0	0	0	0	0	0	0	0	0	0	0	0	0	0	0	0	-1	0	0	0	0
0	0	1	-1	0	0	0	0	0	0	0	0	0	0	0	0	0	0	0	0	0	0	0	0
0	0	0	1	-1	0	0	0	0	0	0	0	0	0	0	0	0	0	0	0	0	1	0	0
0	0	0	0	1	-1	-1	-1	0	0	0	0	0	0	0	0	0	0	0	0	0	0	0	0
0	0	0	0	0	0	1	-1	0	0	0	0	0	0	0	0	0	0	0	0	0	0	0	0
0	0	0	0	0	0	0	1	-1	0	0	0	0	0	0	0	0	0	0	0	0	0	0	0
0	0	0	0	0	1	0	0	1	-1	0	0	1	1	0	0	0	0	0	0	0	0	0	0
0	0	0	0	0	0	0	0	0	1	-1	-1	-1	0	0	0	0	0	0	0	0	0	0	0
0	0	0	0	0	-1	0	0	0	0	0	-1	-1	1	1	2	0	0	0	0	0	0	0	0
0	0	0	0	0	0	0	-1	0	1	0	-1	0	0	0	0	0	0	0	0	0	0	1	1
0	0	0	0	0	0	0	0	0	0	0	0	1	0	0	-1	-1	0	0	0	0	0	0	0
0	0	0	0	0	0	0	0	0	0	0	0	0	0	0	0	0	-1	-1	0	1	0	0	-1
0	0	0	0	0	0	0	0	0	0	0	0	0	0	0	0	0	0	0	0	0	0	-1	1
0	0	0	0	0	0	0	0	0	0	0	0	0	0	0	0	0	0	0	0	0	1	-1	-1
0	1	-1	0	0	0	0	0	0	0	0	0	0	0	0	0	0	0	0	0	0	0	1	1
0	0	0	0	0	0	0	1	0	1	1	0	1	0	0	0	0	-1	1	0	0	0	0	-1

TABLE I

THE STOICHIOMETRIC MATRIX FOR THE GROWTH PHASE.

without loss of generality. The stoichiometric matrix N is presented in Table I, the rows following the same ordering as the list of metabolites: Glucose 6-Phosphate, Dihydroxyacetone Phosphate, Glyceraldehyde 3-Phosphate, Pyruvate, Acetyl-coenzyme A, Citrate, α -ketoglutarate, Malate, Glutamate, Oxaloacetate, Aspartate, Ribose 5-Phosphate, Ribulose 5-Phosphate, Erythrose-4-Phosphate, Xylulose-5-Phosphate, Fructose-6-Phosphate, CO_2 . The vectors coding for the resulting elementary flux modes are shown in Table II. As explained above, from these modes ten macroscopic reactions are obtained by keeping only the initial substrates and final products. For instance, the first mode (i.e. first column in Table II) defines a path in the network made up of arcs $v_1, v_2, v_3, v_4, v_5, v_6$ that connect Glucose to Lactate. This gives a macroscopic reaction (in moles):

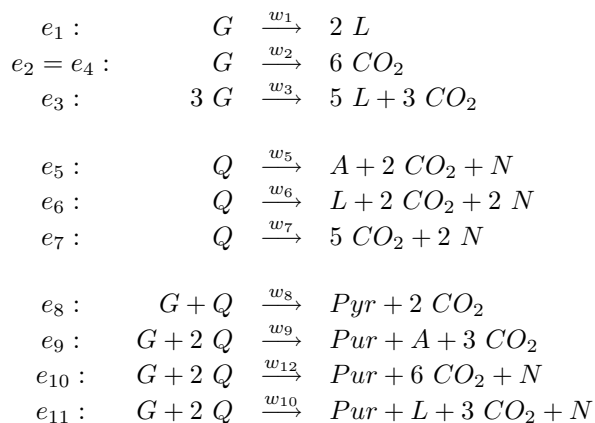


with the stoichiometric coefficients given by entry (1,1) of $N_s E$ for Glucose and entry (1,1) of $N_p E$ for Lactate with:

$$N_s = \begin{pmatrix} v_1 & v_{16} & v_{17} & v_{18} & v_{24} \\ -1 & \dots & 0 & 0 & 0 & \dots & 0 \\ 0 & \dots & 1 & 1 & 2 & \dots & 0 \end{pmatrix}$$

$$N_p = \begin{pmatrix} v_1 & v_6 & v_7 & v_{14} & v_{15} & v_{24} \\ 0 & \dots & 1 & 0 & \dots & 0 & 0 & \dots & 0 \\ 0 & \dots & 0 & 1 & \dots & 0 & 0 & \dots & 0 \\ 0 & \dots & 0 & 0 & \dots & 1 & 1 & \dots & 0 \end{pmatrix}$$

The ten macro-reactions for the growth are as follows:



where G, Q, L, N, A stand for Glucose, Glutamine, Lactate, Ammonia and Alanine respectively. Leaning on the above

	e_1	e_2	e_3	e_4	e_5	e_6	e_7	e_8	e_9	e_{10}	e_{11}
v_1	1	1	3	3	0	0	0	1	1	1	1
v_2	1	1	0	0	0	0	0	0	0	0	0
v_3	1	1	2	2	0	0	0	0	0	0	0
v_4	1	1	2	2	0	0	0	0	0	0	0
v_5	2	2	5	5	0	0	0	0	0	0	0
v_6	2	0	5	0	1	0	0	0	0	0	1
v_7	0	0	0	0	0	1	0	0	1	0	0
v_8	0	2	0	5	0	0	1	0	0	1	0
v_9	0	2	0	5	0	0	1	0	0	1	0
v_{10}	0	2	0	5	0	0	1	0	0	1	0
v_{11}	0	2	0	5	1	1	2	1	2	3	2
v_{12}	0	2	0	5	0	0	1	1	1	2	1
v_{13}	0	0	0	0	1	1	1	0	1	1	1
v_{14}	0	0	0	0	0	0	0	1	1	1	1
v_{15}	0	0	0	0	1	0	1	0	0	1	1
v_{16}	0	0	0	0	1	1	1	0	0	0	0
v_{17}	0	0	0	0	0	0	0	0	1	1	1
v_{18}	0	0	0	0	0	0	0	1	0	0	0
v_{19}	0	0	3	3	0	0	0	1	1	1	1
v_{20}	0	0	1	1	0	0	0	1	1	1	1
v_{21}	0	0	2	2	0	0	0	0	0	0	0
v_{22}	0	0	1	1	0	0	0	0	0	0	0
v_{23}	0	0	1	1	0	0	0	0	0	0	0
v_{24}	0	6	3	18	2	2	5	2	3	6	3

TABLE II

THE ELEVEN ELEMENTARY FLUX MODES FOR THE GROWTH PHASE

described formalism, the growth model is written as:

$$\dot{\xi}_g = \underbrace{\begin{pmatrix} -1 & -1 & -3 & -3 & 0 & 0 & 0 & -1 & -1 & -1 & -1 \\ 0 & 0 & 0 & 0 & -1 & -1 & -1 & -1 & -2 & -2 & -2 \\ 2 & 0 & 5 & 0 & 0 & 1 & 0 & 0 & 0 & 0 & 1 \\ 0 & 0 & 0 & 0 & 1 & 2 & 1 & 0 & 0 & 1 & 1 \\ 0 & 0 & 0 & 0 & 1 & 0 & 0 & 0 & 1 & 0 & 0 \end{pmatrix}}_{K_g} wX$$

with:

$$\xi_g = \begin{pmatrix} G \\ Q \\ L \\ N \\ A \end{pmatrix}$$

The ten reactions are distributed in three groups depending on the used substrate:

- reactions e_1, e_2, e_3 with Glucose substrate;
- reactions e_5, e_6 and e_7 with Glutamine substrate;
- reactions e_8 to e_{11} with both Glucose and Glutamine substrates.

In order to further reduce the size of the model, the reactions of each group are then aggregated into a single reaction.

$$f_1 = \alpha_1 e_1 + \alpha_2 e_2 + (1 - \alpha_1 - \alpha_2) e_3$$

$$f_2 = \beta_1 e_5 + \beta_2 e_6 + (1 - \beta_1 - \beta_2) e_7$$

$$f_3 = \frac{1}{2} e_8 + \frac{\gamma_1}{2} e_9 + \frac{\gamma_2}{2} e_{10} + \frac{1 - \gamma_1 - \gamma_2}{2} e_{11}$$

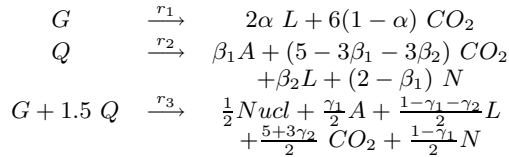
The aggregation matrix A_g is therefore composed of three columns which entries contain unknown parameters. There are three, three and four parameters respectively representing the weight of each macro-reaction e_i in the resulting aggregated reactions. However these parameters are constrained by the fact that the entries of a column of A_g should sum up to one and consequently the number of unknowns in a column is obtained as the number of aggregated reactions

minus one. Moreover, the Purine and Pyrimidine nucleotides are assumed to be produced at the same rate because DNA and RNA are made up with equal shares of these two species (which are therefore lumped into a single species denoted Nucl). This explains the particular form of the third aggregated reaction and why there are only two parameters in the third column of A_g .

The corresponding aggregation matrix is:

$$A_g = \begin{pmatrix} \alpha_1 & 0 & 0 \\ \alpha_2 & 0 & 0 \\ 1 - \alpha_1 - \alpha_2 & 0 & 0 \\ 0 & 0 & 0 \\ 0 & \beta_1 & 0 \\ 0 & \beta_2 & 0 \\ 0 & 1 - \beta_1 - \beta_2 & 0 \\ 0 & 0 & \frac{1}{2} \\ 0 & 0 & \frac{\gamma_1}{2} \\ 0 & 0 & \frac{\gamma_2}{2} \\ 0 & 0 & \frac{1 - \gamma_1 - \gamma_2}{2} \end{pmatrix}$$

The three aggregated reactions are:



with $\alpha = \alpha_1 + \frac{5}{2}\alpha_2$

The reduced mass balance model for the growth phase can now be written as:

$$\dot{\xi}_g = \underbrace{\begin{pmatrix} -1 & 0 & -1 \\ 0 & -1 & -1.5 \\ 2\alpha & \beta_2 & \frac{1 - \gamma_1 - \gamma_2}{2} \\ 0 & (2 - \beta_1) & \frac{1 - \gamma_1}{2} \\ 0 & \beta_1 & \frac{\gamma_1}{2} \end{pmatrix}}_{L_g = K_g A_g} \underbrace{\begin{pmatrix} r_1 \\ r_2 \\ r_3 \end{pmatrix}}_{r_g} X$$

In this model, the pseudo stoichiometric matrix L_g is full rank ($rank(L_g) = 3$) independently of the values of the parameters. Furthermore, there are at most two unknown parameters in each column of L_g . According to Theorem 2 in [4], this proves that the parameters $\alpha, \beta_i, \gamma_i$ ($i=1,2$), are structurally identifiable from the experimental data, without the knowledge of the specific reaction rates r_i .

A more detailed presentation of the parameter estimation procedure can be found in [4]. From the data depicted in Fig. 3, we have obtained the following parameter values:

$$\alpha = 0.99, \beta_1 = 0.2, \beta_2 = 0.8, \gamma_1 = 0.8, \gamma_2 = 0.2.$$

The reactions rates of the three aggregated reactions are modelled by Michaëlis-Menten kinetics:

$$\begin{aligned} r_1 &= \mu_1 \frac{G}{k_G + G} \\ r_2 &= \mu_2 \frac{Q}{(k_Q + Q)} \\ r_3 &= \mu_3 \frac{GQ}{(k_G + G)(k_Q + Q)} \end{aligned}$$

In order to complete the model, it remains to select numerical values for the parameters μ_i, k_G and k_Q . Under the balanced growth condition, it clearly makes sense to assume that the macro-reactions proceed almost at their maximal rate during the exponential growth phase. The half-saturation constants k_G and k_Q are therefore selected small enough to be ineffective during the growth phase but large enough to avoid stiffness difficulties in the numerical simulation of the model. Here we have set the half-saturation constants at the following values:

$$k_G = k_Q = 0.1 mM.$$

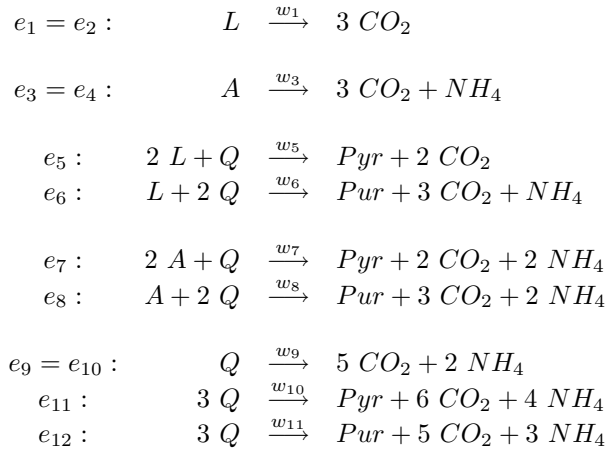
Finally, a simple empirical fitting gives the following values for the μ_i parameters:

$$\mu_1 = 0.1652, \mu_2 = 0.0234, \mu_3 = 0.0192$$

The growth model obtained with these values has been used to produce the simulation results presented in Fig. 4. Obviously, the model succeeds in describing the concentration of the CHO cells measured metabolites during the growth. However, for the remainder of the cell life, the cell behaviour is clearly different and is wildly overshoot by the simulation.

B. The Transition Phase Model

Now that an efficient model is available for the growth, a different metabolic network is depicted in Fig. 5 for the transition phase which occurs in the time period just after Glucose is exhausted (from about 80 to 120h). As we can see in Fig. 3, during this period the cells keep growing while Lactate and Alanine start to be consumed. Our assumption is then to consider Lactate and Alanine as new substrates, in addition to Glutamine whose consumption is slowed down. Therefore, some of the reactions of the previous network are inverted in order to be in agreement with this assumption and, in particular, to still have a production of the nucleotide precursors. For this network, there are nine elementary flux modes. The following nine macro-reactions are subsequently derived:



The matrix K_t is easily obtained:

$$K_t = \begin{pmatrix} 0 & 0 & 0 & 0 & -1 & -2 & -1 & -2 & -1 & -1 & -3 & -3 \\ -1 & -1 & 0 & 0 & -2 & -1 & 0 & 0 & 0 & 0 & 0 & 0 \\ 0 & 0 & 1 & 1 & 0 & 1 & 2 & 2 & 2 & 2 & 4 & 3 \\ 0 & 0 & -1 & -1 & 0 & 0 & -2 & -1 & 0 & 0 & 0 & 0 \end{pmatrix}$$

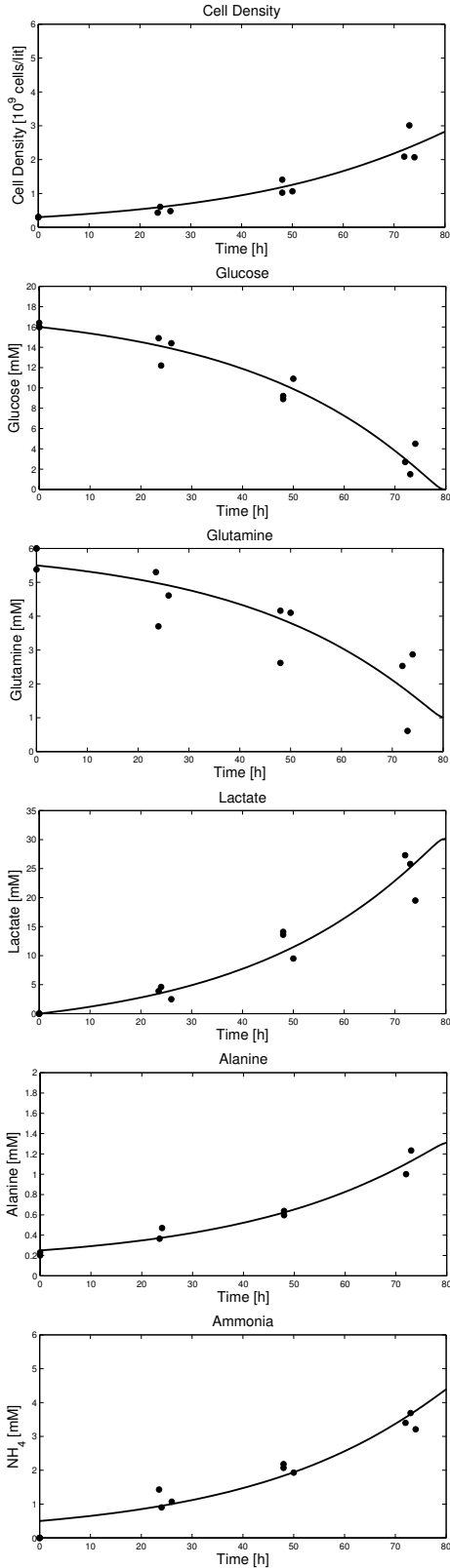


Fig. 4. Simulation resulting from the growth phase model.

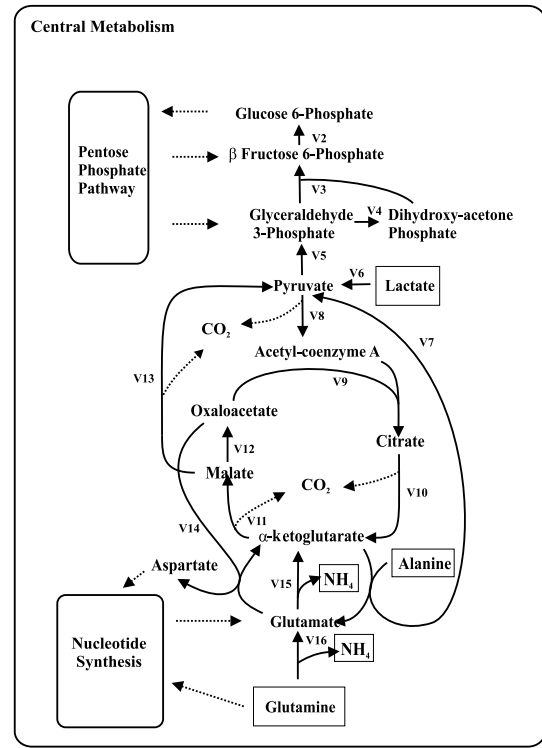


Fig. 5. Metabolic network proposed for the transition phase.

Then, as above, the macroscopic reactions that share the same reactants are aggregated:

$$\begin{aligned}
 f_1 &= e_1 \\
 f_2 &= e_3 \\
 f_3 &= \frac{1}{2}(e_5 + e_6) \\
 f_4 &= \frac{1}{2}(e_7 + e_8) \\
 f_5 &= \gamma_1 e_9 + \left(\frac{1-\gamma_1}{2}\right)(e_{11} + e_{12})
 \end{aligned}$$

with the aggregation matrix:

$$A_t = \begin{pmatrix}
 1 & 0 & 0 & 0 & 0 & 0 \\
 0 & 0 & 0 & 0 & 0 & 0 \\
 0 & 1 & 0 & 0 & 0 & 0 \\
 0 & 0 & 0 & 0 & 0 & 0 \\
 0 & 0 & 0 & \frac{1}{2} & 0 & 0 \\
 0 & 0 & 0 & \frac{1}{2} & 0 & 0 \\
 0 & 0 & 0 & 0 & \frac{1}{2} & 0 \\
 0 & 0 & 0 & 0 & \frac{1}{2} & 0 \\
 0 & 0 & 0 & 0 & 0 & \gamma_1 \\
 0 & 0 & 0 & 0 & 0 & 0 \\
 0 & 0 & 0 & 0 & 0 & \frac{1-\gamma_1}{2} \\
 0 & 0 & 0 & 0 & 0 & \frac{1-\gamma_1}{2}
 \end{pmatrix},$$

in order to obtain a reduced set of five normalized macro-

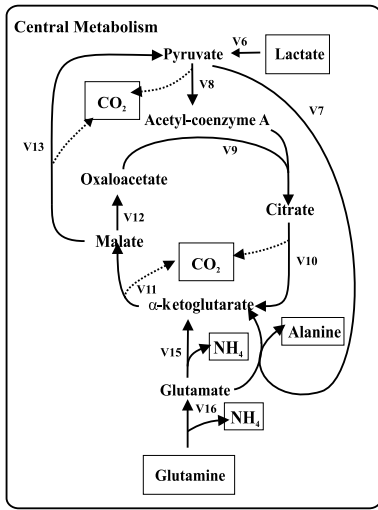
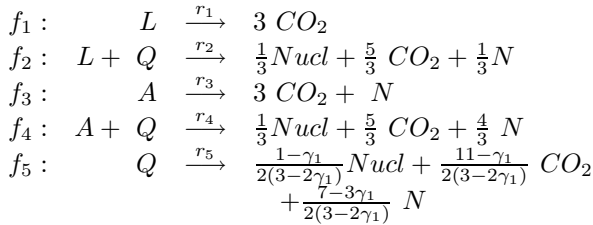


Fig. 6. Metabolic network for the death phase.

reactions:



Finally, the transition phase model is written as follows:

$$\dot{\xi}_t = L_t r_t X$$

where

$$\xi_t = \begin{pmatrix} Q \\ L \\ N \\ A \end{pmatrix} \text{ and } L_t = \begin{pmatrix} 0 & -1 & 0 & -1 & -1 \\ -1 & -1 & 0 & 0 & 0 \\ 0 & \frac{1}{3} & 1 & \frac{4}{3} & \frac{7-3\gamma_1}{2(3-2\gamma_1)} \\ 0 & 0 & -1 & -1 & 0 \end{pmatrix}.$$

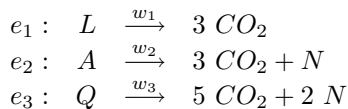
Again, Michaëlis-Menten kinetics are used:

$$\begin{aligned}
 r_1 &= \mu_1 \frac{L}{k_L + L} & \mu_1 &= 0.0345 \\
 r_2 &= \mu_2 \frac{LQ}{(k_L + L)(k_Q + Q)} & \mu_2 &= 0 \\
 r_3 &= \mu_3 \frac{A}{k_A + A} & \mu_3 &= 0.0005 \\
 r_4 &= \mu_4 \frac{AQ}{(k_A + A)(k_Q + Q)} & \mu_4 &= 0.0008 \\
 r_5 &= \mu_5 \frac{Q}{k_Q + Q} & \mu_5 &= 0 \\
 & & \gamma_1 &= 1
 \end{aligned}$$

and $k_L = k_A = k_Q = 0.1mM$.

C. The Death Phase Model

During the death phase, it is assumed that the nucleotides are no longer produced. The metabolic network (Fig. 6) has then been modified to satisfy that assumption. The only three deduced macroscopic reactions having three different substrates, this macro-reactions set is not reduced any further.



The macroscopic reaction rates are modelled by Michaëlis-Menten kinetics:

$$\begin{aligned}
 r_1 &= \mu_1 \frac{L}{k_L + L} & \mu_1 &= 0.0348 \\
 r_2 &= \mu_2 \frac{LQ}{k_A + A} & \mu_2 &= 0.0011 \\
 r_3 &= \mu_3 \frac{Q}{k_Q + Q} & \mu_3 &= 0.0002
 \end{aligned}$$

and : $k_L = k_A = k_Q = 0.1mM$. The death phase model is formulated as follows:

$$\dot{\xi}_d = L_d r_d X$$

with

$$\xi_d = \begin{pmatrix} Q \\ L \\ N \\ A \end{pmatrix} \text{ and } L_d = \begin{pmatrix} 0 & 0 & -1 \\ -1 & 0 & 0 \\ 0 & 1 & 2 \\ 0 & -1 & 0 \end{pmatrix}$$

D. The Complete Model

In order to finally achieve complete modelling of the cell life, the three models obtained above are used successively. The transition between them is achieved by smoothly switching from model to model. In practice, the complete model is a superposition of the three models whose respective influence is controlled by means of weighting functions noted ϕ_g , ϕ_t and ϕ_d respectively for the growth, transition and death phases. The final model is formulated as follows:

$$\begin{aligned}
 \dot{\xi} &= \phi_g \dot{\xi}_g + \phi_t \dot{\xi}_t^* + \phi_d \dot{\xi}_d^* \\
 &= \phi_g K_g r_g + \phi_t K_t^* r_t + \phi_d K_d^* r_d
 \end{aligned}$$

where these vectors and matrices

$$\xi_t^* = \begin{pmatrix} 0 \\ \xi_t \end{pmatrix}, \xi_d^* = \begin{pmatrix} 0 \\ \xi_d \end{pmatrix}, K_t^* = \begin{pmatrix} 0 \\ K_t \end{pmatrix}, K_d^* = \begin{pmatrix} 0 \\ K_d \end{pmatrix},$$

are augmented in order for the three models to fit in the same framework.

The weighting functions were taken as being functions of time, sliding from 0 to 1 for particular values of the Glucose and Glutamine substrates. When there is enough Glucose, only the growth model is activated. With the progressive exhaustion of Glucose, the function ϕ_g passes from 1 to 0 meaning that the influence of this model begins to fade out. Then the transition model progressively gets into action with the passage of ϕ_t from 0 to 1. The same mechanism controls the second transition but this time, it is triggered by Glutamine reaching a threshold value. ϕ_d switches smoothly from 0 to 1 while the value of ϕ_t returns to 0. As the transition model effect dampens, the death model takes over for the remainder of the cell life.

The switching functions are represented in Fig. 7. Note

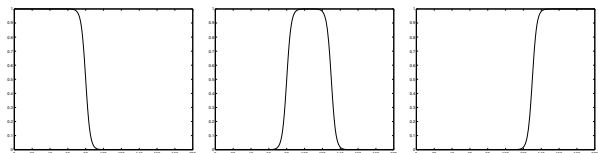


Fig. 7. The smooth switching functions: ϕ_g , ϕ_t and ϕ_d

that this kind of model structure based on smooth switching between local models has been previously considered in e.g. [5].

IV. CONCLUSION

The simulation results show that the cell life can be modelled by a succession of well chosen simple metabolic networks. An entire and complex dynamical modelling of the biochemical pathways is not needed in order to achieve macroscopic modelling. However the knowledge contained therein provides a substantial base to build up a macroscopic model.

V. ACKNOWLEDGMENTS

This paper presents research results of the Belgian Programme on Interuniversity Attraction Poles, initiated by the Belgian Federal Science Policy Office. The scientific responsibility rests with its authors. The authors gratefully acknowledge the contribution of National Research Organization and reviewers' comments.

REFERENCES

- [1] CH. Schilling, S. Schuster, BO. Palsson and R. Heinrich, Metabolic Pathway Analysis: Basic Concepts and Scientific Applications in the Post-Genomic Era., *Biotechnol Prog.*, vol. 15, 1999, pp 296-303.
- [2] A. Provost and G. Bastin, Dynamic Metabolic Modelling under the Balanced Growth Condition, *Journal of Process Control*, vol. 14, 2004, pp 717-728.
- [3] J.E. Haag, A. Vande Wouwer and P. Bogaerts, Dynamic Modeling of Complex Biological Systems: A Link Between Metabolic and Macroscopic Description, *Mathematical Biosciences*, vol. 193, 2005, pp 25-49.
- [4] G. Bastin and L. Chen, Structural Identifiability of the Yield Coefficients in Bioprocess Models When the Reaction Rates Are Unknown, *Mathematical Biosciences*, vol. 132, 1996, pp 35-67.
- [5] T. A. Johansen and B. A. Foss, Operating Regime Based Process Modeling and Identification, *Computers and Chemical Engineering*, vol. 21, 1997, pp. 159-176.

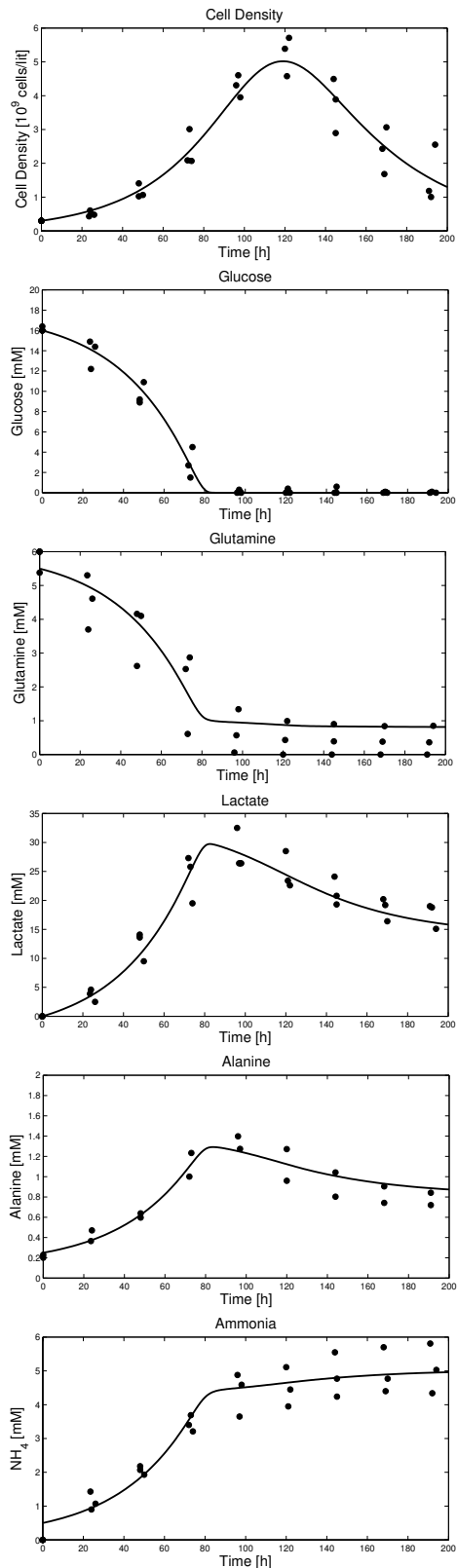


Fig. 8. Simulation resulting from the complete model